IIETA International Information and Engineering Technology Association
Advancing the World of Information and Engineering

Mathematical Modelling of Engineering Problems
Vol. 10, No. 3, June, 2023, pp. 1003-1010
Journal homepage: http://iieta.org/journals/mmep

Experimental Investigation of Thermo-Fluid Characteristics in Air Flow Through Corrugated Tubes with Various Configurations

Salwa Ahmad Sarow[1], Saad Najeeb Shehab[2*]

[1] Department of Environmental Engineering, College of Engineering, Mustansiriyah University, Baghdad 10047, Iraq
[2] Department of Mechanical Engineering, College of Engineering, Mustansiriyah University, Baghdad 10047, Iraq

Corresponding Author Email: saadnajeeb16@uomustansiriyah.edu.iq

https://doi.org/10.18280/mmep.100334

Received: 24 October 2022
Accepted: 12 March 2023

Keywords:
corrugated tube, thermo-fluid, interrupted, forced convection, experimental simulation

ABSTRACT

Engineering and industrial applications, such as heat exchangers, cooling systems, and solar collectors, require designs that optimize heat transfer rates and enhance thermal performance. Corrugated tubes present a viable solution for these applications. In this study, an experimental simulation method was employed to examine the thermo-fluid characteristics of air flow through a one-start horizontally spiraled corrugated tube under turbulent forced convection. A parametric investigation was carried out for various configurations of spirally corrugated tubes subjected to uniform heat flux. Three distinct types of spirally corrugated tubes were investigated: Continuous corrugated tubes with 6mm pitch, continuous corrugated tubes with 18mm pitch, and interrupted corrugated tubes with 6mm pitch. Additionally, a smooth tube was examined for comparison. All tubes were fabricated from copper, and the corrugations were created through cold forming. The effects of air velocity and wall heat flux on flow and heat transfer rates were analyzed, with five air velocities (ranging from 2.5 to 4.5m/s) and six surface heat fluxes (ranging from 5,000 to 10,000W/m^2) considered. Results revealed that the average Nusselt number for the interrupted corrugated tube was 72.5% higher than the smooth tube, 63.5% higher than the corrugated tube with an 18mm pitch, and 12.5% greater than the corrugated tube with a 6mm pitch.

1. INTRODUCTION

Corrugated tubes are a vital heat transfer enhancement technique that minimizes the heat exchange area required, thus reducing costs [1]. By increasing turbulence severity, corrugated pipes enhance heat dissipation [2]. Combining features of fins, extended surfaces, obstructions, and roughness, these tubes have various engineering and industrial applications such as heat exchangers, cryogenics, flat plate collectors, food industries, nuclear reactors, radiators, and cooling systems like R410 floor-standing split air conditioner units [2, 3].

Numerous studies have employed numerical simulations to investigate flow in corrugated channels and tubes to improve thermal performance and flow properties. Researchers like [4] Ozbolat et al. [4], Chorak et al. [5], and HashimYousif [6] used a two-dimensional model and the finite volume method (FVM) to simulate flow and heat transfer through corrugated tubes with different geometries (pitch and corrugation depth). They found that an increase in corrugation depth led to improved thermal performance.

Other researchers used a three-dimensional model for corrugations. Kareem et al. [7] studied the heat transfer improvement rate in a 2-started spirally corrugated tube numerically. They employed computational fluid dynamics (CFD) for water flowing at low Reynolds numbers in helical corrugated tubes and compared it with a plain tube. Their results showed the best heat performance (1.8 to 2.3) with Reynolds numbers ranging from 100 to 700, and heat transfer rates improved by about 21.7% to 60.5%.

Smaisim [8] investigated the convective heat augmentation in corrugated tubes using a four-started spiral numerically. Using ANSYS-Fluent version 14.0, Reynolds numbers ranging from 300 to 1500, different severity indices, and constant wall heat flux, their results indicated heat transfer improvements from 6.15% to 33.3%. Additionally, they observed an increase in friction factor values from 1.8 to 2.93 times compared to smooth tube values. The corrugation with a severity index of 4.76×10-2 had the maximum Nusselt number, and Smaisim also developed a correlation equation to predict the Nusselt number of the four-started helically corrugated tube.

Ajeel et al. [9] simulated the effect of corrugation geometries on flow and heat transfer properties in trapezoidal corrugated channels. They used the finite volume technique to evaluate the continuity, momentum, and energy equations and four different types of nanofluids (Al_2O_3, CuO, SiO_2, and ZnO-water) with a fixed surface heat flux at 10 kW/m^2. Their results showed that corrugation forms significantly impacted heat performance compared with plain profiles. They also observed that, for all shapes, the nozzle rib type of trapezoidal corrugated channels achieved the highest performance.

Abbas [10] conducted an investigation on the forced convective heat transfer rate and pressure drop with various corrugated channel configurations. They used ANSYS-Fluent software to compute turbulent flow and heat behavior for different corrugated channel configurations. With various Reynolds numbers (6000-20000) and a surface heat flux of 6000 W/m^2, they investigated seven trapezoidal corrugation

channel shapes in three groups. They found that the 2FIC type had the highest friction factor and heat transfer rate compared to the other types. They also demonstrated that laminar flow was more valuable than turbulent flow.

Dhaidan and Abbas [11] studied the inward-outward turbulence forced convective heat flow with varied rib-forms using a computational model with different types of corrugations (rectangular, semicircular, and trapezoidal ribs). They alternately placed the corrugation tube ribs in an inward-outward configuration (IOCT) and compared the thermal and hydrodynamic performance of IOCT with inward-rib (ICT), outward-rib (OCT), and smooth tubes. They found that IOCT exchanged heat more effectively than OCT but at the cost of higher pumping power losses. The heat transfer of IOCT was determined to be 17.7% higher than that of OCT at the highest Reynolds number, and IOCT reduced the friction factor by approximately 27.2%.

Kaood et al. [12] investigated the thermo-hydraulic performance of turbulent flow in corrugated tubes numerically. They used the finite volume approach with the k-ε turbulence model and water as a working fluid in an axisymmetric corrugated tube model with a 10mm internal diameter and various roughness geometries. They also employed a fixed wall heat flux condition and seven Reynolds numbers ranging from 5000 to 61000.

The researchers observed that the Nusselt number of trapezoidal, rectangular, curved, and triangular corrugated tubes is greater than that for smooth tubes by about 52.6%, 50.2%, 47.8%, and 45%, respectively. Nfawa et al. [13] conducted a numerical investigation on heat transfer improvement in corrugated trapezoidal channels using winglet-shaped vortex generators. They considered four different heights (1-4mm) and inserted winglet vortex generators at the inlet of each wave with the same slant angle as the trapezoidal channel waves. Reynolds numbers (Re) were utilized to provide consistent heat flow for the lower and upper corrugated walls in the range of 5000 to 17500. They discovered that the longitudinal winglet in the corrugated channel significantly enhances the Nusselt number (Nu) but at the cost of an increased friction coefficient compared to a smooth duct. Furthermore, the winglet longitudinal vortex generator with corrugated ducts is suitable for various types of heat transfer applications.

Boonloi and Jedsadaratanachai [14] simulated the thermal-hydraulic performance enhancement, heat transfer rate, and pressure loss in a duct with a sinusoidal wavy-shaped surface. They employed the finite volume method (FVM) to examine the laminar flow regime at Re values from 100 to 1000. The impact of flow angle of attack (30°, 45°, and 60°) and amplitude ratio (0.10, 0.15, 0.20, and 0.25) on heat transfer and flow structure were analyzed. They observed that the presence of a sinusoidal corrugated surface in a square channel heat exchanger increased the heat transfer coefficient compared to a smooth duct. Moreover, the maximum heat transfer rate using a sinusoidal corrugated surface was found to be approximately 5.5 times higher than a plain surface, with a performance of 1.98.

Kumar and Sharma [15] presented a simulation of heat transfer improvement in corrugated ducts. They used water as the working fluid in a duct with three different corrugation wall shapes: triangular, sinusoidal, and trapezoidal, and considered a wide range of Reynolds numbers with fixed surface heat flux and surface temperatures. They found that the heat transfer improvement in the case of laminar flow is higher for the triangular corrugation channel compared to other channel types and that the pressure drop is lower in the triangular-type channel.

Some researchers, such as Akbarzadeh and Akbarzadeh [16], Zhu et al. [17], and Babapour et al. [18], have experimentally studied turbulent flow in corrugated tubes with different shapes and geometries. They found that the thermal performance of corrugated tubes increases with increasing pitch length and corrugated height, reaching a maximum value of 2.29.

In addition, other researchers, like Gudi and Hindasageri [19, 20], have employed swirl tapes, novel delta tapes, and twisted swirl tapes to generate a swirling airflow. They observed that the swirl flow generators help enhance the heat transfer rate.

From the aforementioned research, most studies have simulated and analyzed corrugations and corrugated tubes numerically. This work, however, focuses on specially manufactured test rigs and the fabrication of corrugated tubes using a single roller cold-forming process to conduct experiments and analyze the thermal characteristics and heat performance of airflow inside one-start spirally corrugated tubes under forced convective conditions. Three different configurations of spirally corrugated tubes—continuous corrugated tubes with a 6mm pitch, continuous corrugated tubes with an 18mm pitch, and interrupted corrugated tubes with a 6mm pitch—are utilized and compared to a smooth tube to determine the best model.

2. EXPERIMENTAL ANALYSIS

2.1 Experimental setup

Figure 1 depicts the custom-designed experimental setup, which is specifically tailored to accommodate diverse test cases for this study. The setup comprises a test section, pipe connections, a valve, a centrifugal air blower, a digital temperature recorder, a multimeter, a voltage regulator, and measuring instruments. As illustrated in Figure 2, the test section encompasses a corrugated copper tube, a heating element, thermocouples, and thermal insulation.

The tubes feature dimensions of 440 mm in length, 35 mm in outer diameter, 32.5 mm in inner diameter, and a 1.25 mm thickness, while the corrugated test section spans 400 mm. As demonstrated in Figure 3, thermocouples are strategically positioned along the length of the corrugated tube. The corrugated tubes were fabricated using a single roller cold forming technique, as illustrated in Figure 4.

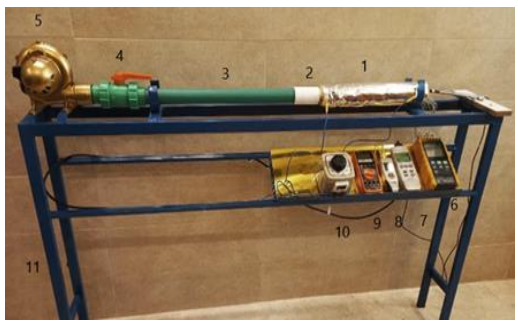

Figure 1. Photograph of setup: 1) Test sections 2) connector 3) fully developed pipe 4) flow control valve 5) air blower 6) digital temperature recorder, 7) anemometer 8) manometer 9) digital multi-meter, 10) voltage regulator 11) steel stand

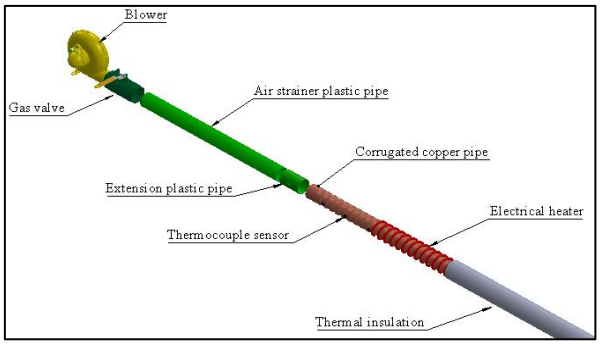

Figure 2. Schematic diagram of setup

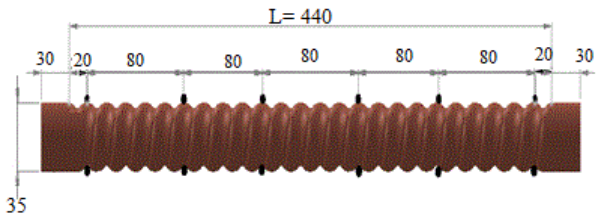

(a) Continuous corrugated tube

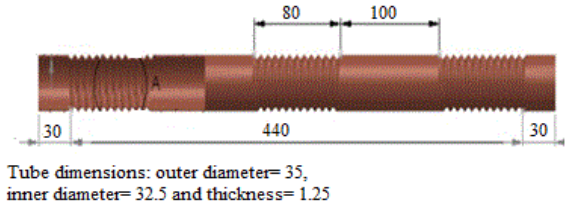

(b) Interrupted corrugated tube

Figure 3. Dimensions (in mm) and thermocouples locations for continuous and interrupted corrugated tubes

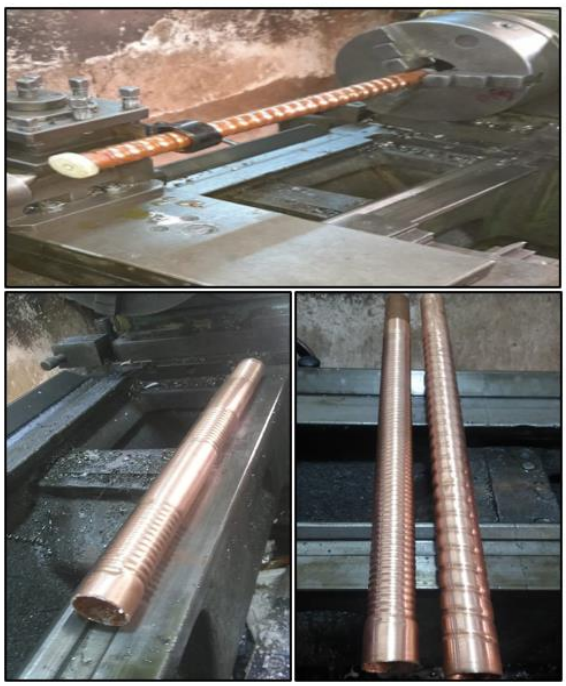

Figure 4. Manufacturing of corrugated tubes models

Three various cases of spirally corrugated tubes like, continuous corrugated tubes with pitch 6mm, continuous corrugated tubes 18mm and interrupted corrugated tube with pitch 6mm in addition, a smooth tube are manufactured and cold formed to experiments as shown in the Figure 5.

Figure 5. Tested copper tubes

2.2 Experimental procedure

The experiments are performed on three cases of corrugated tubes plus smooth tube with different air flow velocities ranging (2.5-4.5m/s) and wall heat fluxes ranging between 5000 and 10000W/m^2 as the following procedures:

(1) The thermocouples are fixed on the outer surface of the tube with a thermal adhesive.
(2) The tube is inserted into the coiled heater and then covered by asbestos with thickness of 10mm and then is covered by 50mm thickness glass wool layer.
(3) After operating the air blower, all connections are inspected to ensure that there is no air leakage.
(4) The air velocity is adjusted by changing the flow control valve to the desired value.
(5) Switched on the power supply, the heater operating, the voltage adjusted using the variable adjustable digital voltage transformer to reach the desired heat flux.
(6) The readings of tube surface temperatures, inlet and outlet air temperatures are recorded when reach steady-state conditions, also the pressure differential Δp readings at the inlet and outlet of tube are recorded.
(7) Steps 3, 4, and 5 are repeated to cover all ranges of air velocity and wall heat fluxes.
(8) Steps from 1 to 7 are repeated for the other cases of helically corrugated tubes and smooth tube.

2.3 Mathematical model

Based on the tubes configurations the data analysis for heat transfer rate and fluid flow is achieved.

2.3.1 Rate of heat transfer

The power input (Q_{in}) to electrical helically heater covered a copper tube can be calculated as follows:

$$Q_{\text{in}} = V \times I \tag{1}$$

The input power is converted to thermal energy and transported into a tube by heat convection (Q_{conv}), heat conduction (Q_{cond}) and heat radiation (Q_{rad}) according to the first law of thermodynamic.

$$Q_{in} = Q_{\text{conv}} + Q_{\text{rad}} + Q_{\text{cond}} \tag{2}$$

The heat radiation losses (Q_{rad}) that occur between the outer surface of tube and ambient are found small because the emissivity of copper is small (ε=0.05). Therefore, the heat radiation losses are neglected. The heat losses by conduction (Q_{cond}) are also neglected because a good insulation with low thermal conduction (0.15W/m. K) is utilized.

The heat convection (Q_{conv}) between the outer surface of tube and the air flow inside tube can be calculated by Newton's law of cooling as [1]:

$$Q_{conv} = h_{av} A_s \left(T_{s,av} - T_b\right) \tag{3}$$

The area of surface plain tube (A_s) can be expressed as:

$$A_s = \pi D L \tag{4}$$

The area of surface corrugated tube (A_s) can be expressed as follows:

$$A_s = \pi D_h L \tag{5}$$

The bulk temperature (T_b) can be calculated by:

$$T_b = \frac{T_{a,i} + T_{a,o}}{2} \tag{6}$$

The average heat transfer coefficient is evaluated as [1]:

$$h_{av} = \frac{q''}{T_{s,av} - T_b} \tag{7}$$

The wall heat flux (q'') was computed by dividing the input power (Q_{in}) on the heat surface area (A_s):

$$q'' = \frac{IV}{A_s} \tag{8}$$

The average Nusselt number can be computed as a function of average heat transfer coefficient, hydraulic diameter and air thermal conductivity as following [2, 3]:

$$Nu_{av} = \frac{h_{av} D_h}{K_a} \tag{9}$$

The hydraulic diameter (D_h) defined as:

$$D_h = D_n = \frac{d_b + d_{en}}{2} \tag{10}$$

where,

V and I are the voltage (V) and current (A) respectively;

$T_{S,av}$ is the average surface temperature of the tube (K);

L is the tube length (m);

D_n is the nominal diameter (m);

d_b is the bore diameter (m);

d_{en} is the envelope diameter (m);

K_a is the air thermal conductivity (W/m. K).

The Reynolds number (Re) is a significant parameter to know the type of fluid flow in to the tube as follows [2, 21]:

$$Re = \frac{\rho_a u_{av} D_h}{\mu_a} \tag{11}$$

where,

ρ_a, μ_a are the air density (kg/m^3) and air dynamic viscosity (kg/m. s) consequently.

u_{av} is average of the inlet air flow velocity (m/s).

The entrance region length *(Le)* through which a fully developed flow can be obtained [3]:

$$L_e = 4.4 D_h Re^{1/6} \tag{12}$$

The local heat transfer coefficient is calculated as follows:

$$h_x = \frac{q''}{T_{s,x} - T_{a,x}} \tag{13}$$

where,

$T_{s,x}$ is the local surface temperature of the helically corrugated tube (K).

$T_{a,x}$ is the local air temperature (K).

The local Nusselt number can be evaluated as follows [3, 21]:

$$Nu_x = \frac{h_x D_h}{K_x} \tag{14}$$

$$Nu_{av} = \frac{1}{L}\int_0^L Nu_L d_x \approx \frac{\sum_{i=1}^{i=6} Nu_i}{6} \tag{15}$$

2.3.2 Fluid flow

The friction factor is an important parameter and can be determined as [21]:

$$f = \Delta p \times \frac{2 \times D_h}{\rho_a u_{av}{}^2 L} \tag{16}$$

The pressure differential (ΔP) is the difference between inlet pressure (P_i) and the outlet pressure (P_o), and can be calculated as follows:

$$\Delta P = \left(P_i - P_o\right) \tag{17}$$

Air characteristics are taken at the mean film temperature (T_f).

2.4 Experimental uncertainties analysis

Errors and uncertainties of current work due to the calibrations, measurements, types of instruments and readings can be evaluated by using (analytical approach). Average Nusselt number (Nu_{av}) is function as [22, 23]:

$$Nu_{av} = f(V, I, \Delta T) \tag{18}$$

Hence, the uncertainties in the average Nusselt number values can be evaluated as follows [22, 23]:

$$e_{Nu_{av}} = \pm\left[\left(\frac{\partial Nu_{av}}{\partial V}e_V\right)^2 + \left(\frac{\partial Nu_{av}}{\partial I}e_I\right)^2 + \left(\frac{\partial Nu_{av}}{\partial \Delta T}e_{\Delta T}\right)^2\right]^{1/2} \quad (19)$$

The errors are:

- Voltage error ($e_V = \pm 0.05$)
- Current error ($e_I = \pm 0.005$)
- Temperature difference error ($e_{\Delta T} = \pm 0.01$)

where,

$$\Delta T = \left(T_{s,av} - T_b\right) \quad (20)$$

$$\left(\frac{\partial \mathrm{Nu}_{av}}{\partial \mathrm{V}}\right) = \left(\frac{\mathrm{ID_h}}{\mathrm{A_S \Delta Tk}}\right) \quad (21)$$

$$\left(\frac{\partial Nu_{av}}{\partial I}\right) = \left(\frac{VD_h}{A_S \Delta Tk}\right) \quad (22)$$

$$\left(\frac{\partial Nu_{av}}{\partial \Delta T}\right) = \left(\frac{VID_h}{A_S (\Delta T)^2 k}\right) \quad (23)$$

Relative error (E_R) can be expressed as follows [21]:

$$E_R = \frac{e_{Nu_{av}}}{Nu_{av}} \quad (24)$$

Maximum relative error in average Nusselt number is about (E_R=0.00045).

2.5 Validation of current data

A comparison between present data than Akbarzadeh and Akbarzadeh work [16] for a case of smooth tube is done as shown in Figure 6. It can be noted that the same behavior, and found the maximum deviation near from (14%) because the different in some work conditions such as values of wall heat flux.

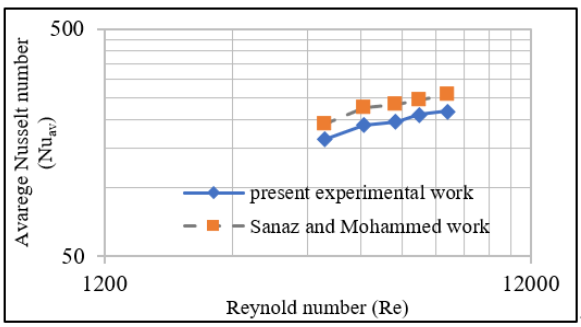

Figure 6. Validation of current data

3. RESULT AND DISCUSSION

Results obtained from the tests of forced convective for air-flow through a various corrugated tubes are analyzed.

3.1 Effect of local Nusselt number

Figure 7 shows the behavior of local Nusselt number along different studied corrugated models tubes and smooth tube at air velocities (2.5 and 4.5m/s), and different heat fluxes (5000 and 10000W/m^2). For all cases, it's noted the local Nusselt number at inlet tube is high value then decreases along the length of the inner tube due to increasing air temperature while moving from inlet to outlet of the tube. The interrupted corrugated tube contributes to the continuous regeneration for the thermal boundary layers, this leads to a reduction in the thermal boundary layer thickness, so the local Nusselt number is greater about (71.5%) than smooth tube and greater about (56%) than corrugated pipe (with pitch 18mm), and about (9.5%) than corrugated pipe (with pitch 6.0mm).

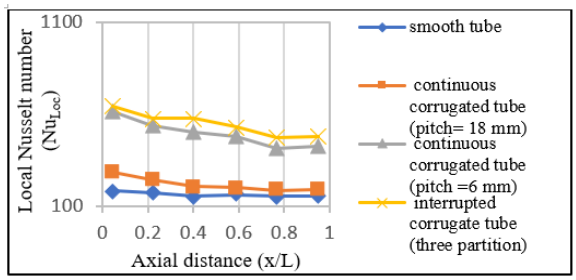

(a) u=2.5m/s, q=5000W/m^2

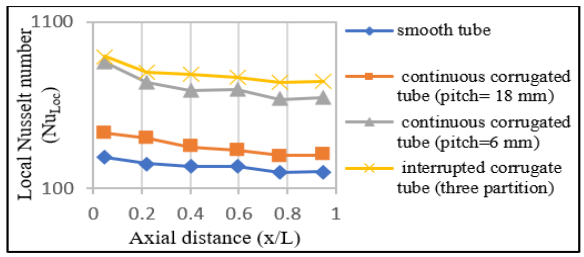

(b) u=4.5m/s, q=10000W/m^2

Figure 7. Influence of the local Nusselt number along axial tube length

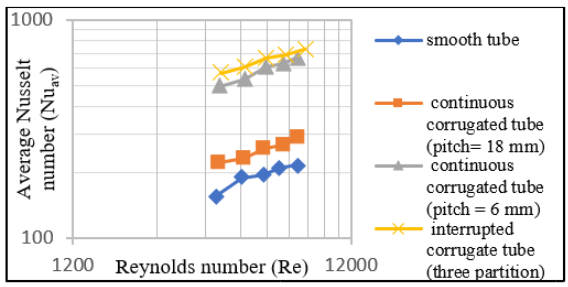

(a) q=5000W/m^2

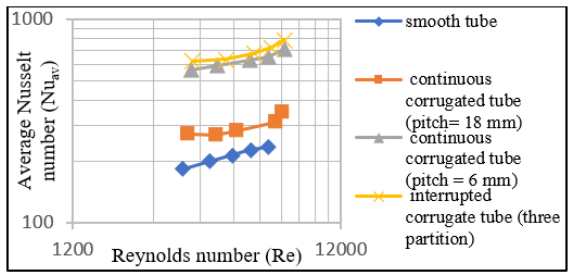

(b) q=10000W/m^2

Figure 8. Behavior of the average Nusselt number against Reynolds number for various tubes cases

3.2 Effect of Reynolds number

The behavior of average Nusselt number (Nu_{av}) against Reynolds number (Re) for various cases of corrugated tubes at different heat fluxes (5000 and 10000W/m^2) is shown in Figure 8. It's noted that the average Nusselt number obtained from experimental results is gradually increased with increasing Reynolds number. This is due to greater boundary layer thickness motivated at low Reynolds number in smooth tube and implementing of corrugations became more active on the flow mixing in this region, while at higher (Re), the boundary layer of smooth tube is thinner and the influence of flow separation and reattachment on the improvement ratio at the wake region of the corrugated tubes are comparatively constant. For interrupted corrugated tube, the average Nusselt number about (72.5%) larger than smooth tube and about (63.5%) larger than corrugated pipe (with pitch 18mm), and about (12%) larger than corrugated pipe (with pitch 6.0mm).

3.3 Effect of average surface temperatures

Variation of average surface temperatures against surface heat flux is illustrated in the Figure 9 at velocities 2.5 and 4.5m/s for different corrugated tubes models. It's clear that the average surface temperatures increase continuously with increasing wall heat flux and decreases with increasing the air flow velocity in the tubes. For smooth tube, the average surface temperature is greater about (11.5%) than corrugated tube of pitch 18mm and about (16%) greater than corrugated tube of pitch 6.0mm and about (19.5%) greater than interrupted corrugated tube. So, the interrupted corrugated tube model can used in the solar heat flat collector or double pipe heat exchangers to increase the performance and decrease the cost.

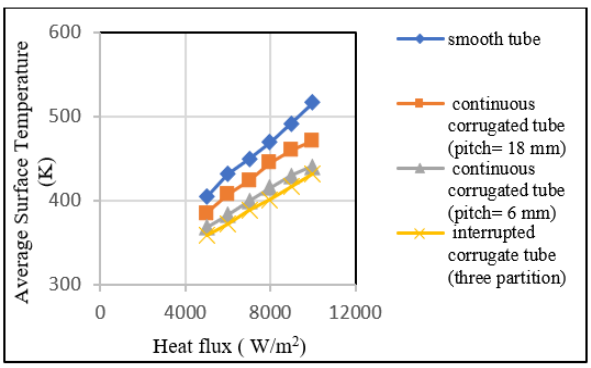

(a) u=2.5m/s

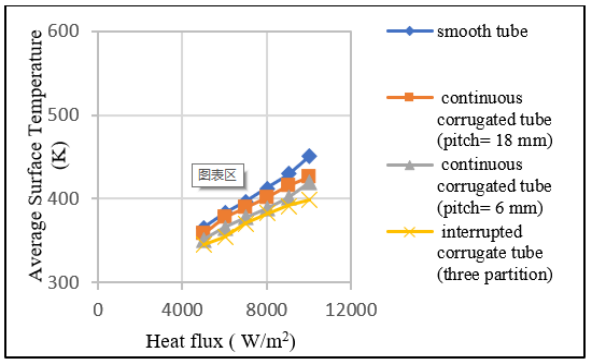

(b) u=4.5m/s

Figure 9. Behavior of friction factor versus Reynolds number at different tubes cases

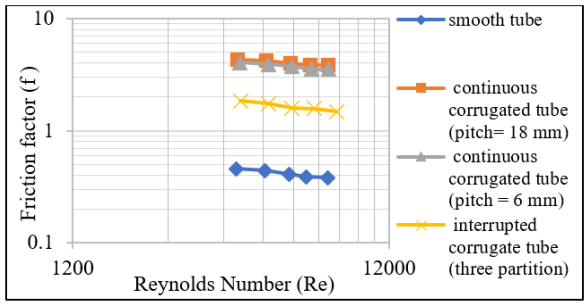

(a) q=5000W/m^2

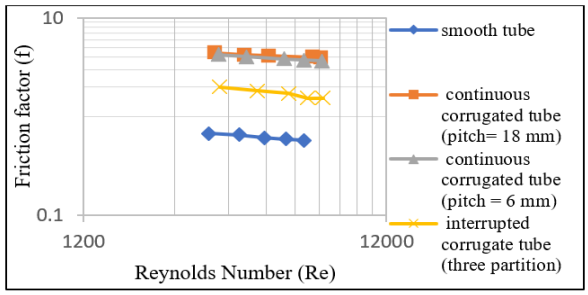

(b) q=10000W/m^2

Figure 10. Behavior of friction factor versus Reynolds number at different tubes cases

3.4 Effect of friction factor

Figure 10 illustrates the behavior of friction factor with Reynolds number at various corrugated and smooth tubes at a different heat flux. It's indicated that the increment in Reynolds number leads to a reduction in the friction factor (for all cases) because the collision between air molecules increases with increasing air velocity, and this leads to a reduction in the values of friction factor. From the experimental work the friction factor of the spirally continuous corrugated tubes with length of pitch (18mm) was observed to be higher than that in the other cases and smooth tube because the flow of air within the tube faces greater obstruction in the continuous corrugated pipe of pitch of (p=18mm) than the other cases.

4. CONCLUSIONS

In the present work, the parameters linked with convection heat dissipation and pressure drop are studied and analyzed through the different models of corrugated tubes (continuous corrugated with pitches 18 and 6mm and interrupted corrugated tube of pitch 6.0mm), in addition, the smooth tube. The importance conclusions can be listed:

- Local Nusselt number (Nu_x) of interrupted corrugated tube about 71.0% greater than smooth tube, 56% and 9.5% than continues corrugated tubes with pitches lengths (p=18mm) and (p=6.0mm) respectively.
- The average Nusselt number of interrupted corrugated tube 72.5% bigger than a smooth tube, 63.5% greater than corrugated tube of pitch (p=18mm) and 12.5% bigger than corrugated tube of pitch (p=6.0mm).
- Average surface temperatures for the smooth tube are about 19.5% greater than interrupted corrugated tube and about (16%) and 11.5% than continues corrugated tubes of pitches (p=6.0mm) and (p=18mm) consecutively.

- The friction factor values of helically continues corrugated tube with pitch length (p=18mm) are higher than smooth and other models of corrugations.
- Values of Nusselt number (local and average) increase with decreasing corrugated pitch (p) and increasing wall heat flux.

ACKNOLEDGMENT

The authors wish to thank Mustansiriyah University (www.uomustansiriyah.idu.iq) Baghdad, Iraq for its support in the present research.

REFERENCES

[1] Calomino, F., Tafarojnoruz, A., De Marchis, M., Gaudio, R., Napoli, E. (2015). Experimental and numerical study on the flow field and friction factor in a pressurized corrugated pipe. Journal of Hydraulic Engineering, 141(11): 04015027. http://doi.org/10.1061/(ASCE)HY.1943-7900.0001046

[2] Tokgoz, N., Aksoy, M.M., Sahin, B. (2017). Investigation of flow characteristics and heat transfer enhancement of corrugated duct geometries. Applied Thermal Engineering, 118: 518-530. https://doi.org/10.1016/j.applthermaleng.2017.03.013

[3] Bergman, T.L., Lavine, A.S., Incropera, F.P. Dewitt, D.P. (2011). Introduction to Heat Transfer, Sixth Edition. Wiley, John & Sons, Incorporated.

[4] Ozbolat, V., Tokgoz, N., Sahin, B. (2013). Flow characteristics and heat transfer enhancement in 2D corrugated channels. International Journal of Mechanical and Mechatronics Engineering, 7(10): 2074-2078. https://doi.org/10.5281/zenodo.1088554

[5] Chorak, A., Ihringer, E., Abdellah, A.B., Dhimdi, S., Essadiqi, E.H., Bouya, M., Faqir, M. (2014). Numerical evaluation of heat transfer in corrugated heat exchangers. In 2014 International Renewable and Sustainable Energy Conference (IRSEC), IEEE, 401-406. http://doi.org/10.1109/IRSEC.2014.7059913

[6] HashimYousif, A. (2015). Numerical analysis for flow and heat transfer in new shapes of corrugated channel. Journal of Babylon University/Engineering Sciences, 23(2): 540-551.

[7] Kareem, Z.S., Jaafar, M.M., Lazim, T.M., Abdullah, S., AbdulWahid, A.F. (2015). Heat transfer enhancement in two-start spirally corrugated tube. Alexandria Engineering Journal, 54(3): 415-422. https://doi.org/10.1016/j.aej.2015.04.001

[8] Smaisim, G.F. (2017). Augmentation of heat transfer in corrugated tube using four-start spiral wall. Al-Qadisiya Journal for Engineering Sciences, 10(4): 451-467. https://doi.org/10.30772/qjes.v10i4.493

[9] Ajeel, R.K., Salim, W.S.I.W., Hasnan, K. (2018). Impacts of corrugation profiles on the flow and heat transfer characteristics in trapezoidal corrugated channel using nanofluids. Journal of Advanced Research in Fluid Mechanics and Thermal Sciences, 49(2): 170-179.

[10] Abbas, A.K. (2018). Numerical study on forced convection heat transfer and pressure drop for different configurations of corrugated channels. Journal University of Kerbala, 16(2): 93-106.

[11] Dhaidan, N.S., Abbas, A.K. (2018). Turbulent forced convection flow inside inward-outward rib corrugated tubes with different rib-shapes. Heat Transfer-Asian Research, 47(8): 1048-1060. https://doi.org/10.1002/htj.21365

[12] Kaood, A., Abou-Deif, T.M., Eltahan, H., Yehia, M.A., Khalil. E.E. (2018). Thermal-hydrolical performance of turbulent flow in corrugated tube. Journal of Engineering and Applied Science, 65: 307-329. https://www.researchgate.net/publication/327175960

[13] Nfawa, S.R., Talib, A.R.A., Masuri, S.U., Basri, A.A., Hasini, H. (2019). Heat transfer enhancement in a corrugated-trapezoidal channel using winglet vortex generators. CFD Letters, 11(10): 69-80.

[14] Boonloi, A., Jedsadaratanachai, W. (2019). Thermo-hydraulic performance improvement, heat transfer, and pressure loss in a channel with sinusoidal-wavy surface. Advances in Mechanical Engineering, 11(9): 1-17. https://doi.org/10.1177/1687814019872573

[15] Kumar, P., Sharma, S. (2019). Simulation of heat transfer enhancement in corrugated channel by numerical investigation. International Journal of Innovative Trends in Engineering (IJITE), 50(01): 16-19.

[16] Akbarzadeh, S., Akbarzadeh, M.S. (2020). Experimental study on the heat transfer enhancement in helically corrugated tubes under the non-uniform heat flux. Journal of Thermal Analysis and Calorimetry, 140: 1611-1623. https://doi.org/10.1007/s10973-020-09385-5

[17] Zhu, S.L., Wang, J.F., Xie, J. (2021). Numerical investigation of the heat transfer characteristics of r290 flow boiling in corrugated tubes with different internal corrugated structures. Mathematics, 9(22): 2969. https://doi.org/10.3390/math9222969

[18] Babapour, M., Akbarzadeh, S., Valipour, M.S. (2021). An experimental investigation on the simultaneous effects of helically corrugated receiver and nanofluids in a parabolic trough collector. Journal of the Taiwan Institute of Chemical Engineers, 128: 261-275. https://doi.org/10.1016/j.jtice.2021.07.031

[19] Gudi, A., Hindasageri, V. (2022). Experimental and numerical heat transfer study of swirling air jet impingement. International Journal of Heat and Technology, 40(4): 1001-1012. https://doi.org/10.18280/ijht.400418

[20] Gudi, A., Hindasageri, V. (2022). Novel method to improve heat transfer rate through delta swirl tape for a swirl jet impingement study. International Journal of Heat and Technology, 40(3): 715-721. https://doi.org/10.18280/ijht.400308

[21] Abbas, A.S., Mohammed, A.A. (2022). Augmentation of plate-fin heat exchanger performance with support of various types of fin configurations. Mathematical Modelling of Engineering Problems, 9(5): 1406-1414. https://doi.org/10.18280/mmep.090532

[22] Fuentes, H., Valencia, A.A. (2022). Comparison of turbulent flow and heat transfer in a rectangular channel with delta wing and winglet type longitudinal vortex generators. International Journal of Heat and Technology, 40(2): 366-374. https://doi.org/10.18280/ijht.400202

[23] Uhía, F.J., Campo, A., Fernández-Seara, J. (2013). Uncertainty analysis for experimental heat transfer data obtained by the Wilson plot method: application to condensation on horizontal plain tubes. Thermal Science, 17(2): 471-487. http://doi.org/10.2298/TSCI110701136U

NOMENCLATURE

A_s	surface area, m^2
d_b	bore diameter, m
d_{en}	envelope diameter, m
D_h	hydraulic diameter, m
D_n	nominal diameter
f	friction factor
h	coefficient of convection heat transfer, $W/m^2.K$
I	current, A
K_a	air thermal conductivity, W/m. K
L_e	entrance region length, m
Nu	Nusselet number
P	pressure, Pa
q″	Wall heat flux, W/m^2
Q_{cond}	conduction heat loss, W
Q_{conv}	forced heat convective, W
Q_{in}	heat input, W
Q_{rad}	radaition heat loss, W
Re	Reynolds number
T_b	bulk temperature, ℃
T_s	surface temperature, ℃
u_{av}	average air velocity, m/s
V	voltage, V

Greek symbols

μ_a	air dynamic viscosity, kg/m.s
ρ_a	air density, kg/m^3

Subscripts

av	average
i	inlet
o	outlet
x	local